

Article

Kinetic Analysis of Additive on Plasma Electrolytic Boriding

Yongfeng Jiang *, Yefeng Bao and Min Wang

College of Mechanical & Electrical Engineering, Hohai University, Changzhou 213022, China; baoyf@hhuc.edu.cn (Y.B.); wangm@hhuc.edu.cn (M.W.)

* Correspondence: jiangyf@hhuc.edu.cn; Tel.: +86-519-8560-8020; Fax: +86-519-8512-0010

Academic Editors: Qi Hua Fan and Thomas Schuelke

Received: 1 March 2017; Accepted: 24 April 2017; Published: 28 April 2017

Abstract: Plasma electrolytic boriding (PEB) is a method of combination surface strengthening and surface texturing on metal. In this study, the kinetics and the lubrication friction of borided layers in the plasma electrolytic boriding on the Q235 were investigated in an aqueous solution for 5–15 min. The cross-section and surface morphologies of the boriding layers were confirmed using scanning electron microscope (SEM). The presence of phases on the surface was determined using the X-ray diffraction. The hardness and the lubrication friction were evaluated using a micro-hardness tester and pin-on-disk friction tester in an oil sliding condition, respectively. The PEB layer contains phases in FeB, Fe₂B, Ni₃B₄, NiB, and Ni₂B. It is indicated that the value of activation energy in the PEB treatment is approximately 186.17 kJ/mol. The random micro-pores in surface texturing are unevenly distributed on the surface of the Q235. The micro-hardness of the boriding layer is up to 900 HV, whereas that of the substrate is approximately 181 HV. The weight loss of PEB sample in 10 min is 0.0017 mg in the lubrication friction, whereas that of untreated sample is 0.0047 mg in the same condition. The formation of boriding strengthening surface texturing in PEB improves lubrication friction greatly.

Keywords: plasma electrolytic boriding; kinetics; morphology; friction

1. Introduction

Boriding is a relatively effective method of improving surface tribology on steel. The conventional boriding processes such as pack or paste boriding, liquid or molten salt boriding, electrochemical boriding, plasma-assisted boriding available for the treatment of engineering components are expensive to use due to high temperature in these treatments [1]. Boriding has been one of the thermochemical processes that has been developed and used recently in industries. The most relevant element of the procedure is the production of very hard layers that can exceed 2000 HV, allowing a better wear strength and abrasion than other thermochemical processes like carburizing and nitriding. During boriding, the diffusion and subsequent reaction of boron atoms with metallic substrate forms interstitial boron compounds. The resulting layer may consist of either a single-phase boride or a poly-phase boride layer. The type of metal under treatment, the boriding method and composition of boriding media, temperature, and time of treatment, play important roles in deciding the quality and disposition of obtained boride layers. In general, the thickness of the boride layer increases with the increase of boriding temperature and time, but varies for different materials under the same boriding conditions. Among all different kinds of boriding methods, only pack boriding has been widely used on a commercial basis. Yet the pack boriding process has the disadvantages of relatively high processing temperature and long process duration for getting an effective boride layer thickness. The plasma electrolytic boriding (PEB) is the integrated outcome of conventional electrolysis and atmospheric plasma process [1,2]. The aqueous solution is heated by applied voltage, which

can produce many bubbles around the electrode, and discharges then emerge as a consequence of expansion and cooling of the bubbles. The entire surface of the electrode in an aqueous solution may be covered by a limited quantity of discrete plasma discharges [2]. The imploded bubble can make boron atoms diffuse into the localized melting surface rapidly, leading to the formation of randomly distributed surface texturing [3–6]. Although smart electrolytic plasma technologies have been studied in the last few years, systematic study on PEB still needs to advance [2].

In the past decades, anode plasma electrolytic boriding of medium carbon steel and high-temperature oxidation of Q235 low-carbon steel treated by plasma electrolytic borocarburing was investigated by S.A. Kusmanov [3] and Bin Wang [4], respectively. The processing mode (850–900 °C, 5 min) of medium carbon steels allowing one to obtain a hardened surface layer of up to 0.11 mm with microhardness 1800 HV and with decrease in the roughness three-fold is proposed. The anode PEB could decrease friction coefficient and increase wear resistance of the medium carbon steel. The PEB/C steels had much lower weight gain than the untreated substrate under isothermal oxidation of 500 °C and 600 °C. The oxidation resistance of PEB/C steel with different thickness of boride layer was similar. At 600 °C, the final weight gain of PEB/C samples is 4–5 times lower than that of bare steel substrate. This was attributed to the formation of the Fe₂B phase with good thermal stability in the boride layer. The thickness and the hardness of the carbon-saturated layer on pure iron for 60 min were 78 µm and 850 HV. It was also demonstrated that the depth of the carburized layer on stainless steel was close to 100 µm and its microhardness was up to 880 HV. The growth kinetics of plasma electrolytic carburizing on pure iron was also investigated by Usta [5]. The thickness of the carburized layer ranged from 20 to 160 µm and the hardness ranged of 550–850 HV. Moreover, plasma electrolytic nitrocarburizing (PEN/C) on stainless steel and low carbon steel was studied as well [6–9]. The electrolyte-electrode interface bonding mechanism and surface characterization were also carried out [6]. Previous studies reveal that the plasma electrolytic saturation technology can improve the overall surface performance on the metal. However, the investigation of the PEB was merely in microhardnesses of 4340, 4140, 1045, 3215, and 1020 steel by M.A. Béjar [10]. The systematic study on the effect of the boriding strengthening surface texturing in PEB on the lubrication friction is yet less.

In this study, the plasma electrolytic boriding (PEB) process on low-carbon Q235 steel was carried out for 5–15 min in an aqueous solution. The kinetics in the PEB was investigated and the activation energy was calculated. The cross-section, surface morphologies, phase compositions, and hardness of the PEB coatings were analyzed. The lubrication friction of surface strengthening texturing on the Q235 was investigated in the oil lubrication conditions.

2. Experimental Details

2.1. Material and Preparation

Q235 samples in a size of 9 mm × 3 mm × 40 mm were polished with alumina emery paper in 800-grit size. Then these samples were cleaned in ethyl alcohol and dried in air. The PEB was carried out in 40 kVA plasma electrolytic pulse power. The samples of Q235 and 304 stainless steel bath were connected to the cathode and anode, respectively. Table 1 shows the nominal compositions of the Q235 steel and the 304 stainless steel. During the processes, the sample was performed in the electrolyte consisted of 20 g/L borax, 5 g/L sodium fluoborate (NaBF₄), 2 g/L nickel sulfate (NiSO₄), 30 mL/L ethylene diamine tetraacetic acid disodium, 10 mL/L glycerinum, and deionized water at applied voltage in the range of 150–250 V with an average current density of 0.6 A/cm² for 5, 10 and 15 min. The experiment was exposed in ambient temperature. After the PEB treatment, the sample was rinsed with deionized water and dried in air. Boriding samples were etched in an alcohol solution containing a 4 v % nitric acid.

Table 1. Nominal compositions of steel.

Steel	C (%)	Si (%)	Mn (%)	P (%)	S (%)	Cr (%)	Ni (%)	Ti (%)	Fe (%)
Q235	0.14–0.22	<0.07	0.30–0.60	<0.045	<0.05	–	–	–	Bal.
304	<0.08	<1.0	<2.0	<0.045	<0.03	18–20	8–12	–	Bal.
GCr15	0.95–1.05	0.15–0.35	0.2–0.4	–	–	1.3–1.65	–	–	Bal.

2.2. Characterization of Boriding Layer

The cross-section and surface morphologies were examined using the scanning electron microscope (SEM). The average thickness values of the boriding layer were calculated using simple arithmetic mean. The phase composition of the boriding layer was identified using X-ray diffractometer with Cu K α radiation (40 kV, 200 mA). The hardness values in cross-section of samples were measured using a micro-hardness tester with a load of 50 g. The lubrication friction of the untreated and PEB samples were compared using MPX-2000 (Chenxin Test Equipment Manufacturer Co., Ltd., Zhangjiakou, China) pin-disk friction under a load of 50 N with friction counterparts GCr15 as showed in Table 1. The quantities of weight loss were measured using electronic balance at a precision of 0.1 mg. The quantities of weight loss were measured every 1000 r in a load of 50 N at the speed of 370 r/min. The diameter of wear was 26.9 mm.

3. Results and Discussions

3.1. Microstructures

Figure 1 illustrates cross-section morphologies of the boriding layer. It can be seen that the countless discharge channels apparently are distributed in the boriding layer and many columnar crystals perpendicular to the surface of the substrate are formed along the discharge direction. The interfaces of the boriding layer and substrate for 10 and 15 min are dense, whereas it is not so dense for 5 min than that of treated more time. The boriding layer inserts the substrate jaggedly for 15 min. It is also indicated that the thickness of boriding layer increases with the processing time.

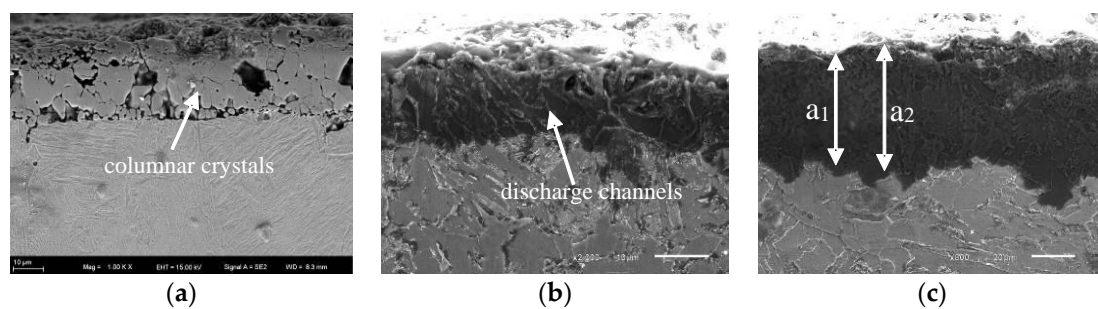


Figure 1. Cross-section morphologies of the PEB layer for (a) 5 min; (b) 10 min; and (c) 15 min.

The thickness of the boriding layer is one of the most important parameters for the kinetics of the boriding layer. The average thicknesses of the boriding layer were calculated using simple arithmetic mean formula (1) [11]. The depths of the boriding layer were calculated as a mean of 11 measurements (only two of them are shown in Figure 1c). According to the computational methods described, the calculated average thicknesses of the boriding layer for 5, 10 and 15 min are 21.28, 24.60 and 27.77 μm , respectively. Due to some defects on surface in microstructures, the boriding coatings are inhomogeneous and PEB occurred firstly on these defective locations. The formation of boride phases and high temperature in the heat-affected zones promote the adsorption of borides in these regions and the transformation of adsorbed boride in layer. Subsequently, micro-zone containing boride formed, which was composed of borides and small micropores. Because micro-zones containing boride are

thicker than the other regions of layer, PEB discharge was difficult in these micro-zones. As a result, the thinner regions are favorable for further PEB discharge. The shift of PEB to thinner regions improved the expansion of micro-zone containing boride. With continuous reactions, a relatively homogeneous boride layer was formed finally.

$$d = \frac{\sum_{i=1}^n a_i}{n} \quad (1)$$

where d is average layer thickness, a_i is random layer thickness, n is numbers. Surface morphologies of the PEB treatment are shown in Figure 2. It is indicated that many micro-pores are unevenly distributed on the surface, exhibiting randomly distributed surface texturing (Figure 2a). The PEB layer consists of a large amount of the nanoparticles, indicating that the formation of nanoparticles is presented in the PEB on Q235 as shown in Figure 2b. Meanwhile, many micro-pores as channels in plasma discharges can be obviously noticed. As processing time continues, micro-melting zones like fish scale are generated on the surface of Q235. Perhaps, the surface texturing of the boriding layer with plentiful anomalous micro-pores has a good effect on oil storage to reduce the friction and wear and improve the surface properties of parts. The porosity observed in the layers made during the PEB process caused the layer to gain a good lubrication that increased the wear strength on the surface.

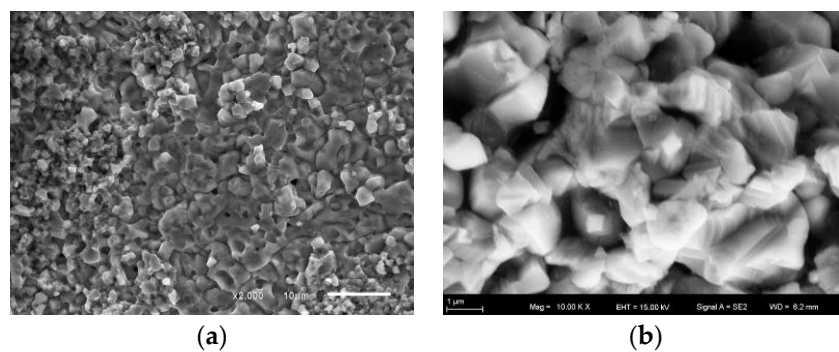


Figure 2. SEM photographs of surface morphologies in the PEB (a) 5 min; (b) 15 min.

3.2. XRD

The phases of the PEB layer are shown in the XRD pattern (Figure 3). The PEB-treated layer consists of boron–nickel compounds and boron–iron compounds in FeB, Fe₂B, Ni₃B₄, NiB, and Ni₂B. Nickel with a higher atomic number than iron, has preferential chemical reaction with boron [12,13]. Meanwhile, iron has chemical reaction with boron under the condition of nickel as a catalyst. The diffusion of nickel has been found in the boriding layer. The boron–iron compounds concentrate below boron nickel compounds and boron–nickel compounds accumulate at the outer surface. In the process of PEB, boride molecules moved towards cathodic surface in electric field. As a result, a high concentration region of borides presented at the interface between cathode and solution. In addition, a concentration gradient of borides was formed in solution from anode to cathode. Therefore, the high chemical potential of borides at sample/solution interface provided a favorable condition for borides adsorption from solution to sample surface. During PEB, borides were formed around the discharge channel under the condition of high temperature produced. Due to the quenching effect in the solution, the borides were solidified immediately and boride phases formed. The active surface of these borides, which possessed abundant surface energy, played a role of adsorptive center. Consequently, in order to reduce surface energy of the new generated phase, borides in solution were adsorbed on these surfaces and an adsorption layer of borides was formed. Furthermore, a heat-affected zone was produced around each discharge channel and its thickness was five times of the diameter of discharge channel. Energy in the zone promotes the diffusion of borides to the inner of borides layer. It was beneficial

to the proceeding of continuous adsorption of borides in the instantaneous high temperature in the heat-affected zone and critical breakdown voltage.

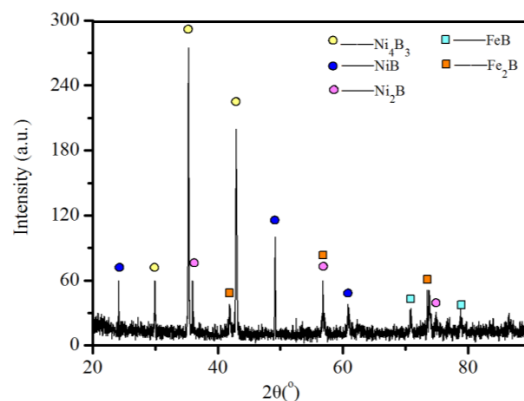


Figure 3. XRD pattern of the PEB-treated Q235.

3.3. Growth Kinetics of Boriding Layer

The boriding atoms must have sufficient energy to overcome an activation energy barrier. The effect of temperature on chemical reaction rates was arrived at by Arrhenius. The relationship between the growth rate constant k , activation energy Q , and the temperature in Kelvin T , can be expressed by Arrhenius equation (Equation (2)) as

$$k = A \exp\left(-\frac{Q}{RT}\right) \quad (2)$$

where A is the diffusion coefficient, Q is the activation energy (J/mol), R is the gas constant, and T is the absolute temperature (K). After a period of PEB time, the interface between the substrate and compact layer was saturated with boron. Figure 4 shows the plot of the square of the thickness of the layer versus the treatment time. The data to different temperatures can be represented by straight lines through the origin. It indicates that the kinetics of boron formation are quite fast. It also clearly indicates that the growing principle of boride layer in all conditions is similar, which is that the layer thickness increases with increasing boriding time. The growth constant was calculated by the slope of the straight lines in Figure 4. The diffusion coefficient of boron has been found in literature [1]. This activation energy is interpreted as the boron diffusion through the direction in the PEB layer. Consequently, the activation energy for the boron diffusion in the PEB layer is determined by the slope, obtained by the plot $\ln d$ versus $1/t$.

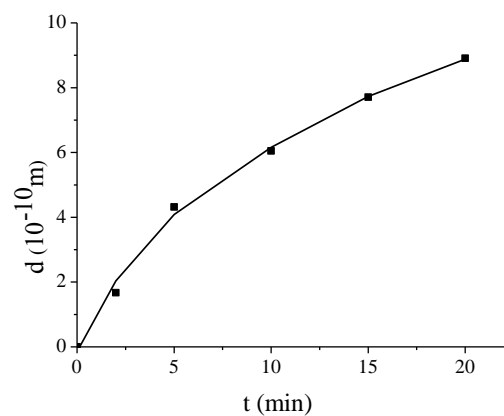


Figure 4. Function of d^2 and t .

Assuming that the boron diffusion obeys a parabolic law [14], the variation of the boriding layer thickness with time can be described as:

$$d^2 = kt \quad (3)$$

where d is the depth of the boriding layer (μm), t is the processing time (s), k is the growth rate constant. The variations of the boriding layer thickness (d^2) at the assuming reaction temperature of 1173 K [11] are shown as a linear function relationship of the boriding time (t) in Figure 4. According to the relationship between d^2 and t , the growth rate constant k was calculated from the slopes of the straight line. Referring to the value of boron diffusion coefficient [12,13], the value of activation energy Q was determined at approximately 186.17 kJ/mol. Therefore, the value of activation energy in the PEB is below than that of the paste boriding processes at an average value of 226.7 kJ/mol [15]. This implies that the PEB can accelerate the diffusion of boride atoms under certain conditions. The PEB can evidently reduce activation energy for the boride diffusion. It is possible that PEB could make the texturing surface more active due to its very high chemical activity, thus accelerating the decomposition rate of boride compounds and adhesion of boride atoms on texturing surface. Therefore, the PEB has a significant enhancement effect on boriding.

3.4. Hardness

Figure 5 shows the variation of the hardness with the distance from surface to center for the untreated and treated samples. It is indicated that the highest value in hardness on the PEB surface is about 900 HV, whereas that of substrate is about 181 HV. It may be due to the presence of the boron–iron compounds and boron–nickel compounds in the boriding layer, implying that the PEB surface have a good tribology. A sharp drop in hardness is presented in the interface between the boriding layer and the substrate. It is possible that no transition layer leads to the large hardness difference between the boriding layer and substrate. The sharp drop for 5 min may be due to excessive corrosion. The hardness of FeB and Fe₂B are up to 1400 HV and 2000 HV, however, the PEB layers under the activation of nickel decrease the value of the hardness and increase the thickness of the boriding layer. A significant role in activation of boron nickel compounds may increase the thickness of the boriding layer. Perhaps the boron mainly manifests solution strengthening leading to the hardness of 900 HV.

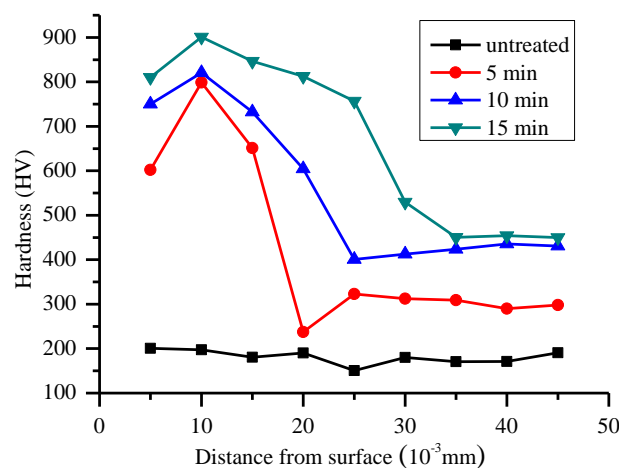


Figure 5. Variation of the hardness with the distance from surface.

3.5. Lubrication Friction Mechanism

The profiles of weight loss with the sliding distance for the treated and untreated samples are shown in Figure 6.

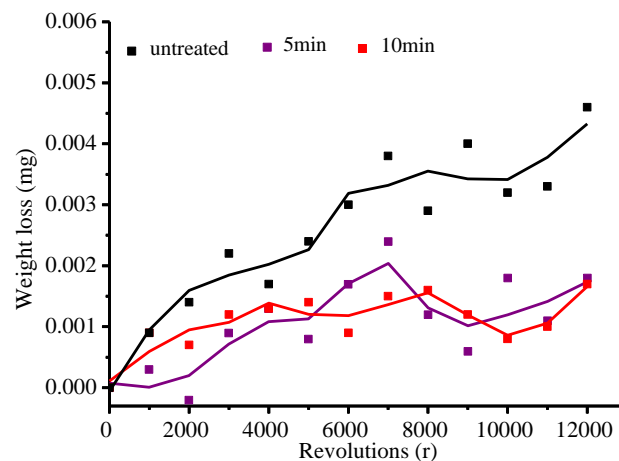


Figure 6. Variation of the weight loss with the revolutions.

Figure 7 illustrates the friction morphologies of the untreated and treated sample. Ploughings and micro cutting grooves appear on the untreated sample as shown in Figure 7a. Abrasive wear on the surface of untreated sample occurs due to the lower hardness of it relative to the counterparts in GCr15. Figure 7b shows that contact fatigue appears on the PEB surface and no ploughings or micro cutting grooves can be seen. It is possible that many uneven micro-pores have a good effect on oil storage to reduce the friction and wear. The hydrodynamic pressure is strongly influenced by the micro-craters and spheroids and the interaction between the micro-craters and spheroids become significant with increasing micro-crater and spheroid area fraction as shown in Figure 8. Because of this interaction, the pressure does not decrease to zero along the width boundary, thereby indicating that the interaction between the micro-craters and spheroids significantly affects the hydrodynamic pressure distribution. During the friction, hydrodynamic pressure is generated in the narrow gap between the mating surfaces. The load carrying capacity can be provided by each micro-craters and spheroids because of an asymmetric hydrodynamic pressure distribution over the micro-craters and spheroids that result from local cavitation in the diverging clearance of the micro-craters and spheroids on the surface also serve as traps for the wear debris and as micro-reservoirs for lubricant retention, thus reducing the ploughing and deformation components of friction and wear. Thus, a combination of unique surface morphology and uniform micro-roughness makes the PEB surface favorable for adhesion to lubricants. A new way is provided to solve the wear and lubrication problem of wear pairs in automobile industry.

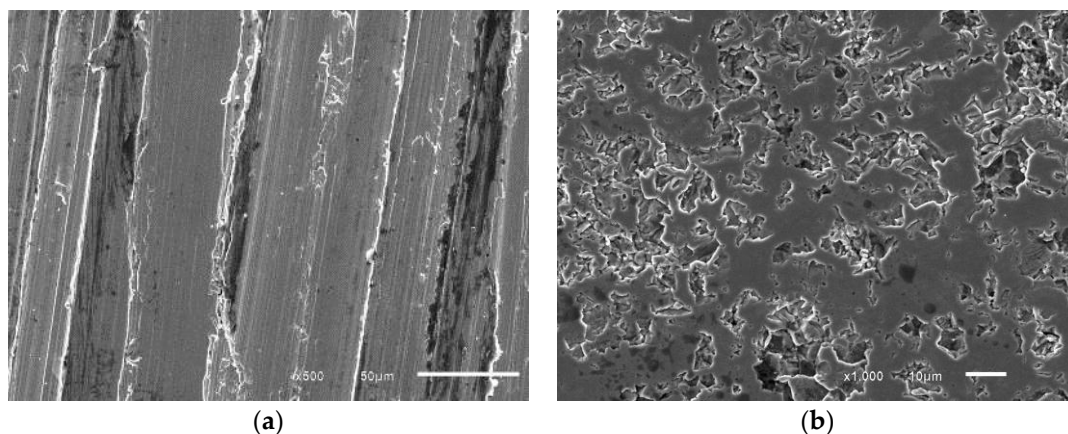


Figure 7. Morphologies of samples (a) untreated; (b) treated for 5 min.

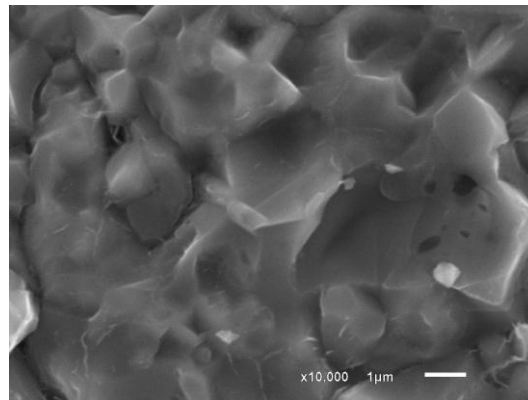


Figure 8. Surface morphology of sample treated for 5 min.

4. Conclusions

The lubrication friction and kinetics of the boriding layers on Q235 were investigated in the plasma electrolytic boriding 20 min. The dependence of growth rate for the boriding layer on the PEB processing time exhibits a parabolic character. The value of activation energy in the PEB treatment is 186.17 kJ/mol. It is below that of the paste or pack boriding processes. The random micro-pores are unevenly distributed in surface texturing on Q235 in the PEB. The highest value in hardness for the PEB surface is about 900 HV, whereas that of substrate is about 181 HV. A sharp drop in hardness is presented in the interface between the boriding layer and the substrate. Ploughings and micro cutting grooves appear on the surface of the untreated sample. The wear mechanisms of the untreated and treated sample are abrasive wear and contact fatigue, respectively. The surface texturing in the PEB on the Q235 can improve lubrication friction.

Acknowledgments: The authors would like to thank the financial support of National Natural Science Foundation of China (No. 50901031) and the Fundamental Research Funds for the Central Universities (No. 2014B11614).

Author Contributions: Yefeng Bao and Yongfeng Jiang conceived and designed the experiments; Min Wang performed experiments; Yongfeng Jiang analyzed the data. Min Wang wrote the paper.

Conflicts of Interest: The authors declare no conflict of interest.

References

1. Parfenov, E.V.; Yerokhin, A.L.; Nevyantseva, R.R.; Gorbakov, M.V.; Liang, C.-J.; Matthews, A. Towards smart electrolytic plasma technologies: An overview of methodological approaches to process modelling. *Surf. Coat. Technol.* **2015**, *269*, 2–22. [[CrossRef](#)]
2. Gupta, P.; Tenhundfeld, G.; Daigle, E.O. Electrolytic plasma technology: Science and engineering—An overview. *Surf. Coat. Technol.* **2007**, *201*, 8746–8760. [[CrossRef](#)]
3. Kusmanov, S.A.; Tambovskiy, I.V.; Sevostyanova, V.S.; Savushkina, S.V.; Belkin, P.N. Anode plasma electrolytic boriding of medium carbon steel. *Surf. Coat. Technol.* **2016**, *291*, 334–341. [[CrossRef](#)]
4. Wang, B.; Wu, J.; Zhang, Y.F.; Wu, Z.L.; Li, Y.L.; Xue, W.B. High-temperature oxidation of Q235 low-carbon steel treated by plasmaelectrolytic borocarburing. *Surf. Coat. Technol.* **2015**, *269*, 302–307. [[CrossRef](#)]
5. Cavuslu, F.; Usta, M. Kinetics and mechanical study of plasma electrolytic carburizing for pure iron. *Appl. Surf. Sci.* **2011**, *257*, 4014–4020. [[CrossRef](#)]
6. Jiang, Y.F.; Geng, T.; Bao, Y.F.; Zhu, Y.H. Electrolyte–electrode interface and surface characterization of plasma electrolytic nitrocarburizing. *Surf. Coat. Technol.* **2013**, *216*, 232–236. [[CrossRef](#)]
7. Nie, X.; Tsotsos, C.; Wilson, A.; Yerokhin, A.L.; Leyland, A.; Matthews, A. Characteristics of a plasma electrolytic nitrocarburising treatment for stainless steels. *Surf. Coat. Technol.* **2001**, *139*, 135–142. [[CrossRef](#)]

8. Wang, B.; Xue, Y.L.; Wu, J.; Jin, X.X.; Hua, M.; Wu, Z.L. Characterization of surface hardened layers on Q235 low-carbon steel treated by plasma electrolytic borocarburing. *J. Alloys Comp.* **2013**, *578*, 162–169. [[CrossRef](#)]
9. Kong, J.H.; Okumiya, M.; Tsunekawa, Y.; Takeda, T.; Yun, K.Y.; Yoshida, M.; Kim, S.G. Surface modification of SCM420 steel by plasma electrolytic treatment. *Surf. Coat. Technol.* **2013**, *232*, 275–282. [[CrossRef](#)]
10. Béjar, M.A.; Henríquez, R. Surface hardening of steel by plasma-electrolysis boronizing. *Mater. Des.* **2009**, *30*, 1726–1728. [[CrossRef](#)]
11. Kartal, G.; Eryilmaz, O.L.; Krumdick, G.; Erdemir, A.; Timur, S. Kinetics of electrochemical boriding of low carbon steel. *Appl. Surf. Sci.* **2011**, *257*, 6928–6934. [[CrossRef](#)]
12. Taheri, P.; Dehghanian, C.; Aliofkhaezai, M.; Rouhaghdam, A.S. Evaluation of nanocrystalline microstructure, abrasion, and corrosion properties of carbon steel treated by plasma electrolytic boriding. *Plasma Process. Polym.* **2007**, *4*, 711–716. [[CrossRef](#)]
13. Badini, C.; Gianoglio, C.; Pradelli, G. The effect of carbon, chromium and nickel on the hardness of borided layers. *Surf. Coat. Technol.* **1987**, *30*, 157–180. [[CrossRef](#)]
14. Campos, I.; Bautista, O.; Ramírez, G.; Islas, M.; De La Parra, J.; Zúñiga, L. Effect of boron paste thickness on the growth kinetics of Fe₂B boride layers during the boriding process. *Appl. Surf. Sci.* **2005**, *243*, 429–436. [[CrossRef](#)]
15. Genel, K. Boriding kinetics of H13 steel. *Vacuum* **2006**, *80*, 451–457. [[CrossRef](#)]



© 2017 by the authors. Licensee MDPI, Basel, Switzerland. This article is an open access article distributed under the terms and conditions of the Creative Commons Attribution (CC BY) license (<http://creativecommons.org/licenses/by/4.0/>).